Frequency and Phase Mixed Coding in SSVEP-Based Brain–Computer Interface

Chuan Jia, Xiaorong Gao, *Member, IEEE*, Bo Hong, *Member, IEEE*, and Shangkai Gao*, *Fellow, IEEE*

***Abstract*—Frequency coding has been the traditional method implemented in steady-state visual evoked potential (SSVEP)-based brain–computer interfaces (BCI). However, it is limited in terms of possible target numbers and, consequently, inappropriate for certain applications involving liquid crystal display (LCD) with multiple stimuli. This paper proposes an innovative coding method for SSVEP that, through a combination of frequency and phase, increases the number of targets, thus it improves the information transfer rate (ITR). With this method, a BCI system with 15 targets was developed using three stimulus frequencies, which is five times as many targets as the traditional method. Additionally, this paper defines the concept of reference phase, and decodes the EEG by means of Fourier coefficient projections onto the reference phase directions. Through the optimization of lead position, reference phase, data segment length, and harmonic components, the average ITR exceeded 60 bits/min in a simulated online test with ten subjects.**

***Index Terms*—Brain–computer interfaces (BCI), frequency coding, phase coding, steady-state visual evoked potential (SSVEP).**

I. Introduction

A BRAIN–COMPUTER interface (BCI) is a direct communication channel [1] between the brain and the outside world. By extracting EEG features, identifying brain's commands and transferring to external-controlled instruments, BCI can be used for helping movement disabled patients to establish a new channel of direct communication between brain and outside world, thus improve their life quality. Due to well-known advantages of simple system configuration, short training time, as well as high-information transfer rate (ITR), the steady-state visual evoked potential (SSVEP)-based BCI has become one of the most promising modalities for a practical noninvasive BCI system [2]–[4].

SSVEP is a response signal of the visual cortex to an outside flicker stimulus at a frequency higher than 6 Hz, which is usually most pronounced in the occipital region of the scalp. SSVEP-based BCI systems typically adopt frequency as the modulation carrier, and set different frequencies for different flickers. However, as SSVEP has a good response only within a limited frequency band, adopting frequency modulation alone restricts the number of targets. Furthermore, when the flickers are shown on the liquid crystal display (LCD), as the stimulus frequency is limited by the refresh rate of the display, the lack of available modulation frequencies become even more serious. Realizing more targets under limited frequencies poses a big challenge for the design of a practical SSVEP-based BCI.

In recent years, phase information in SSVEP has been attracting attention from BCI researchers. Kluge *et al.* [5] and Wilson *et al.* [6] introduced phase information in an SSVEP-based BCI to improve the target identification accuracy. Actually, phase information can play a significant role not only in signal recognition, but also in signal modulation. In an earlier study, Wang *et al.* [7] demonstrated the feasibility of phase modulation in SSVEP. On this basis, this paper further investigates the application of frequency and phase mixed coding in an SSVEP-based BCI.

The BCI system presented in this paper realized 15 targets using three frequencies. In order to recognize the target chosen by BCI users, we propose the concept of reference phase and decode EEG by means of Fourier coefficient projections onto the reference phase directions. To select the most suitable configuration for the system, the following parameters were optimized: the leads, the reference phase, the data segment length, and the number of harmonics. The optimized configurations can be used in future online experiments.

II. Methods

A. EEG Experiment

A total of ten subjects participated in the experiment. Their ages ranged between 22 and 32 years. All of them had normal or corrected to normal vision. Subjects had a clear understanding of the experiment and agreed to participate by signing a consent form before participating in the study.

The experiment was carried out in a normal room without electromagnetic shielding. The subjects were seated in a comfortable armchair, 60 cm away from the stimulation unit.

The EEG data were recorded with a Biosemi Active 2 amplifier at a sampling rate of 256 Hz. The offline experiment used 10–20 electrode caps and recorded 32 channels of EEG. The electrodes' layout was mainly concentrated on the occipital region. The reference electrode and ground electrode were both located at the top of the head, close to each other, near Cz.

Manuscript received April 4, 2010; revised June 23, 2010, and July 31, 2010; accepted August 1, 2010. Date of publication August 19, 2010; date of current version December 17, 2010. This work was supported in part by the National Natural Science Foundation of China under Grant 30630022 and Grant 90820304 and in part by National Basic Research Program of China (973 Program) under Grant 2011CB933204. *Asterisk indicates corresponding author.*

C. Jia, X. Gao, and B. Hong are with the Department of Biomedical Engineering, Tsinghua University, Beijing 100084, China (e-mail: jiachuan@mails.tsinghua.edu.cn; gxr-dea@tsinghua.edu.cn; hongbo@tsinghua.edu.cn).

*S. Gao is with the Department of Biomedical Engineering, Tsinghua University, Beijing 100084, China (e-mail: gsk-dea@tsinghua.edu.cn).

Color versions of one or more of the figures in this paper are available online at http://ieeexplore.ieee.org.

Digital Object Identifier 10.1109/TBME.2010.2068571

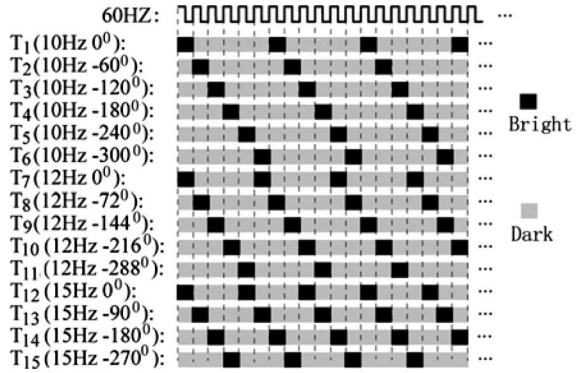

Fig. 1. Flickering sequence for each stimulus.

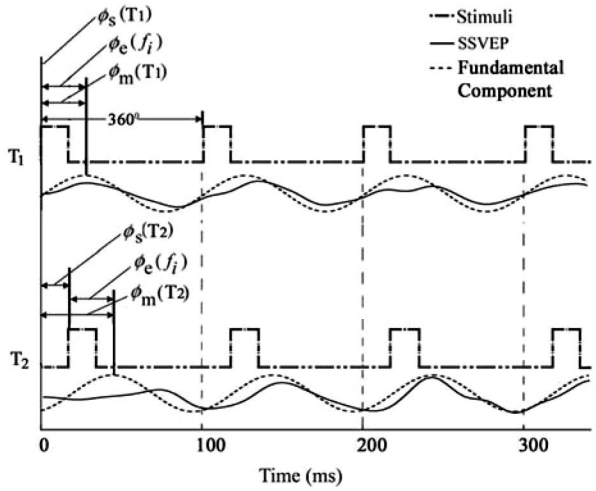

Fig. 2. Relationship of stimulus and SSVEP. In the graphic, s stands for stimuli, e stands for evoked potential, and m stands for measured potential.

B. Stimulation Unit

The system used a ViewSonic VE175 LCD display to present stimuli. The screen had a resolution of 1024 H $\times$ 768 V pixels; and a refresh rate of 60 frames per second. The stimulus flickers were controlled by a computer through a control program written in VC++ based on Windows DirectX API. A total of 15 stimuli were shown on the screen during the experiment. Three different flickering frequencies were used: six stimuli at 10 Hz with a 60° phase difference between neighboring stimuli, five stimuli at 12 Hz with a 72° phase difference between neighboring stimuli, and four stimuli at 15 Hz with a 90° phase difference between neighboring stimuli. Each stimulus was presented in a 100 $\times$ 100 pixels square and the spacing between stimuli was 100 pixels.

The flickering of stimuli was synchronized with the screen refreshing. To enable the flickering of stimuli, the flash block lightening was completed within fixed intervals among frames of screen refresh [8]. The dark and bright sequences of 15 flickers denoted by T_k $(k = 1, 2, \ldots, 15)$ are shown in Fig. 1.

C. Phase Definition

The BCI system presented in this paper is based on mixed coding of frequency and phase. Understanding the underlying mechanisms requires the knowledge of both the relevant signal processing and neurophysiology theory [9]. In this section, we illustrate how the mixed coding system works by going from the stimulus to the SSVEP.

Fig. 2 shows two independent stimuli (T_1 and T_2), and their corresponding SSVEP. These two stimuli have the same frequency (10 Hz), but different phases (0° and −60°).

In what follows, we give a detailed description of the various signals produced, measured, and calculated in this experiment as well as the mathematical notations used in the system.

1) Stimulus Phase $\phi_s(T_k)$: The *stimulus phase*, which is denoted by $\phi_s(T_k)$, describes the relative onsets of stimuli at the same frequency. In Fig. 1, we define the stimulus phase of stimuli T_1, T_7, and T_{12} to be zero degrees for frequencies of 10, 12, and 15 Hz, respectively. The time point, when T_1, T_7, and T_{12} light simultaneously, will be the reference for phase analysis. On this basis, for each of other stimuli, its associated stimulus phase is then designed as the phase difference between its onset and the onset of the stimulus that has the same stimulus frequency and 0° phase. For example, in Fig. 2, $\phi_s(T_1) = 0°$ and $\phi_s(T_2) = -60°$.

2) SSVEP Phase $\phi_e(f_i)$: SSVEP is a periodic response under repetitive stimuli. In general, after every flash, we could observe a waveform, which is phase-locked with the flash. This phase value locked with a stimulus is defined as *SSVEP phase*. Because SSVEP appears after the stimulus, we limited the value of SSVEP phase within 0–360°. In Fig. 2, the SSVEP phase of fundamental component is denoted by $\phi_e(f_i)$ (f_i is the stimulus' frequency).

3) Response Latency $\tau_{\mathrm{res}}(f_i)$: The SSVEP at a certain cycle is not necessarily, a response to the current flash due to the delay in visual information processing. SSVEP latency ranges from 80 to 160 ms [10]–[12]. If the stimulus frequency is small enough (the period is long enough), latency could be clearly identified after each stimulus as a simple transient response. However, if the stimulus frequency is too high (the period is too short), latency may be longer than one period.

Suppose the observed response in each period of SSVEP was evoked by the stimulus, which occurred either in the cycle or a previous cycle, the *response latency* $\tau_{\mathrm{res}}(f_i)$ could then have following relationship with SSVEP phase:

$$\tau_{\mathrm{res}} = \frac{-\left(\phi_{\mathrm{e}}\left(f_i\right) - q \times 360°\right)}{360°} \times \frac{1}{f_i} \tag{1}$$

where f_i is the stimulus' frequency, and q is a integer number, which could be 0, 1, 2,. . ..

4) Measured Phase $\phi_m(T_k)$: The *measured phase*, denoted by $\phi_m(T_k)$, is the measured SSVEP phase in EEG experiment with respect to 0° of stimulus phase. During the experiment, the phases of Fourier coefficients of the fundamental components for each target T_k are obtained with the fast Fourier transform (FFT)

$$\phi_m\left(T_k\right) = \arg\tan\left(\frac{\mathrm{Re}(\mathrm{FFT}(f))}{\mathrm{Im}(\mathrm{FFT}(f)}\right) \quad -360° < \phi_m\left(T_k\right) \leq 0° \tag{2}$$

where

$$\mathrm{FFT}(f) = \frac{1}{\Delta t}\int_{t-\Delta t/2}^{t+\Delta t/2} x(\tau)\exp(\mathrm{j}2\pi f\tau)\mathrm{d}\tau \qquad (3)$$

where f is frequency and Δt is the length of data segment for FFT calculation.

In this study, the data segment for each FFT calculation starts from the onset of the stimuli with zero degree of stimulus phase. In Fig. 2, the measured phase of fundamental component is noted by $\phi_m(T_k)$.

The measured phase of harmonic components can be defined in similar way. However, throughout this article, unless otherwise specified, the measured phase will refer to the fundamental components.

5) Reference Phase $\phi_r(T_k)$: Because the measured phases were calculated from real-EEG recordings, the results differ slightly from time to time. The average of all the measured phases for a specific target T_k is called *reference phase*, and denoted by $\phi_r(T_k)$.

The reference phases were usually calculated in preliminary experiments, as will be described in the following section. The reference phase is one of the most important parameters for the target detection; plus it allows different subjects to use the BCI system.

6) Stimulus Phase Difference $\Delta\phi_s(f_i)$: Phase difference between two stimuli with neighboring phases (e.g., T_1 and T_2 in Fig. 2) under the same frequency is called *stimulus phase difference*, denoted by $\Delta\phi_s(f_i)$.

For example, in Fig. 2, T_1 and T_2 are two stimuli with neighboring phases under 10 Hz, $\Delta\phi_s(10\ \mathrm{Hz}) = 60^\circ$.

7) Measured Phase Difference $\Delta\phi_m(f_i)$: The difference between measured phases when a subject watches two stimuli in adjoining phases (e.g., T_1 and T_2 in Fig. 2) under the same frequency, respectively, is called *measured phase difference*, denoted by $\Delta\phi_m(f_i)$. Ideally, measured phase difference of a fundamental component is close to the stimulus phase difference.

8) Reference Phase Difference $\Delta\phi_r(f_i)$: The difference between reference phases of two stimuli in adjoining phases (e.g., T_1 and T_2 in Fig. 2) under the same frequency is called *reference phase difference*, denoted by $\Delta\phi_r(f_i)$.

D. Phase Clustering in BCI Systems

Under normal condition, individual SSVEP latency is stable [13], [14]. Thus, BCI can discriminate phases evoked by stimuli at different phases with the same frequency. Fig. 3 shows the clustering of measured phases of SSVEP fundamental components evoked by stimuli of different phases at 15 Hz. The stimulus phases are 0°, -90°, -180°, and -270°, respectively. The four radials in Fig. 3 indicate reference phases of different stimuli. From Fig. 3, it can be seen that SSVEPs evoked by stimuli with the same frequency, but different phases cluster in different regions of the complex plane.

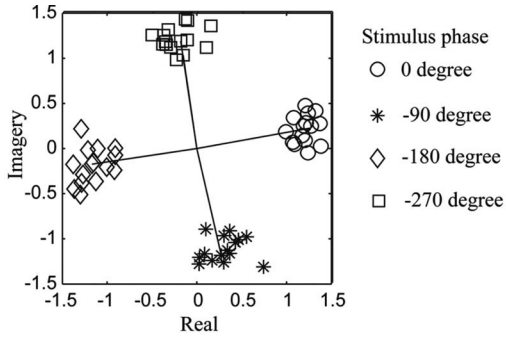

Fig. 3. Measured and reference phases (radials) evoked by stimuli of different phases at 15 Hz. Data come from a subject with different trials. The marks indicate the measured phases when the subject looks at stimuli with different phases.

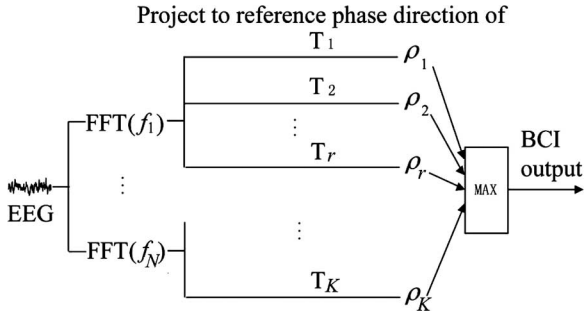

Fig. 4. Discrimination flow of frequency and phase mixed coding signal. In our setup, there are three stimuli frequencies ($N = 3$), and 15 targets ($K = 15$).

E. Decoding Method for the Frequency and Phase Mixed Coding Signals

BCI systems based on SSVEP usually adopt frequency for information coding. Since signals evoked by stimuli with different phases at the same frequency are separable, information can also be coded by the mixing of frequency and phase.

This combination of frequency and phase allows a decoding method based on the amplitude and phase characteristics of EEG at different stimulus frequencies. The decoding scheme is as follows: 1) get the reference phase of each stimulus target; 2) carry out FFT on the EEG signal and obtain the corresponding Fourier coefficient at each stimulus frequency; 3) project the Fourier coefficient at each stimulus frequency onto the reference phase directions; and 4) select the target with maximum projected value as the subject's target (see Fig. 4).

Actually, the proposed decoding method in Fig. 4 contains the analysis of both amplitudes and phases of EEG Fourier coefficients. On the one hand, targets with different frequencies have different Fourier coefficient amplitudes; on the other hand, targets with the same frequency, but different stimulus phases have equal Fourier coefficient amplitude, but different phases. By identifying the maximum amplitude of the Fourier coefficients, the BCI user's intended target will be identified, as it corresponds to the reference phase at the same frequency, which is the closest to the phase of the Fourier coefficient. In Fig. 5, it can be observed that the amplitude of the Fourier coefficient at 15 Hz is the highest one [see Fig. 5(a)] and its phase is closest

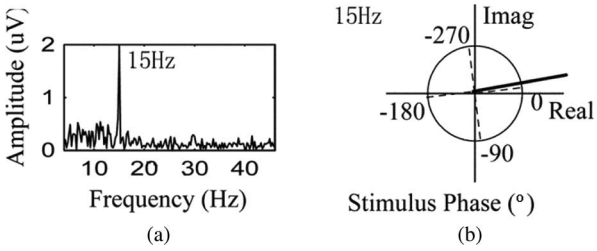

Fig. 5. Decoding method of frequency and phase mixed coding. Data comes from a time section of a subject. (a) Amplitude spectrum. (b) Reference phase of fundamental component at 15 Hz. The dotted line represents the reference phase, the solid line represents the unit circle and axes, the digits around the circle indicate the stimulus phases, and the thick solid line represents the Fourier coefficient.

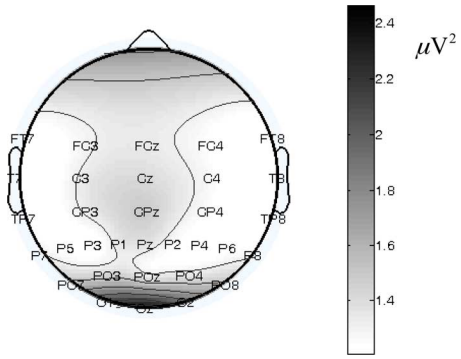

Fig. 6. Energy distribution on scalp.

to the reference phase corresponding to the 0° stimulus at 15 Hz [see Fig. 5(b)]. Therefore, it can be inferred that the BCI user targeted at the flash block of 0° phase with a flickering frequency of 15 Hz.

The second and the third harmonic components of SSVEP can also be introduced into the decoding procedure through reference phase. The decoding method at the second and the third harmonic is similar to that of the fundamental component. In other words, the decoding method projects the second and third harmonic Fourier coefficients onto their reference phase directions as decoding features. The sum of projected lengths of all harmonics' components is the final feature for classification, as shown in the following:

$$\rho_k = \rho_k^1 + \rho_k^2 + \rho_k^3 \qquad k = 1, 2 \ldots K. \tag{4}$$

In the aforementioned formula, the subscript k indicates the stimulus target, and the superscript 1, 2, and 3 indicate the harmonics, respectively. $K = 15$ indicates the total number of targets.

F. Offline Experiment

A total of ten subjects were recruited in the offline experiment. Each of them was required to finish 15 experimental sessions. Each session contained 15 trials and each trial lasted for 6 s with a 2-s pause between flickering stimuli. In the pause, a red cross appeared at one flash block. From seconds 2 through 6, all the flash blocks flickered simultaneously, but the subjects were asked to concentrate on the flash block with the red cross. Within a session, the red cross appeared at each flash block randomly without repetition. The whole experiment lasted for about 30 min.

The EEG recording of the first three sessions was used as the preliminary experiment. In the analysis of offline data, we first carried out the lead position optimization and reference phase calculation using data from the preliminary experiment. Second, results of the preliminary study were used later for the target detection of each experimental session. The choice of a suitable data segment length and harmonic components [15] was also studied in the offline experiment.

TABLE I
OPTIMAL BIPOLAR LEAD

Lead	s1	s2	s3	s4	s5	s6	s7	s8	s9	s10
Signal	Oz	Oz	Oz	Oz	Oz	Oz	Oz	Oz	Oz	OZ
Ref.	POz	POz	POz	PO_3	PO_4	PO_4	PO_3	POz	PO_4	PO_4

III. RESULTS

A. Lead Position

The SSVEP is mainly found in the occipital region of the brain. Fig. 6 shows the distribution of total energy from first three harmonics averaged over all subjects' trials [16].

The independent component analysis (ICA) method proposed for BCI applications by Wang *et al.* [3] was employed to select the optimal bipolar lead for each subject. The optimal bipolar lead obtained in our experiment is shown in Table I.

For all subjects, the lead with maximum signal was the Oz electrode in the occipital region. The reference lead was not in the exact same location for all subjects, but all reference leads were located in the parietal area. For simplicity, we used POz at the center of the parietal area as the reference lead for general use, although it was not the optimal selection for some subjects. A postprocessing study indicated that the choice of the Oz–POz bipolar lead for all subjects induces little influence on SNR compared to the optimal selection.

B. Reference Phase

The preliminary experiment allowed the computation of reference phases for each target. As explained in Section II, the reference phase is the average of the measured phases. Ideally, the difference between two measured phases and corresponding stimulus phases at same frequency should be identical. For example, if the stimulus phase difference at 15 Hz is 90°, the measured phase difference at 15 Hz should also be 90°. However, this may not occur in reality, since external factors also affect the brain waves. Table II compares the measured phase difference with the stimulus phase difference. It shows the number of trials from ten subjects, the stimulus phase difference ($\Delta\phi_s$), and the normal fitting of the measured phase difference ($\Delta\phi_m$) with the mean and standard deviation.

In general, the reference phase difference is close to the stimulus phase difference. Ideally, the reference phases within the

TABLE II
IDEAL VERSUS EMPIRICAL REFERENCE PHASES

Harmonic	Frequency	Number of trials	ϕ_s (°)	Mean of ϕ_m (°)	Standard deviation of ϕ_m (°)
Fundamental	10Hz	180	60	60	29
	12Hz	150	72	72	22
	15Hz	120	90	90	17
Second	10Hz	180	120	118	54
	12Hz	150	144	144	59
	15Hz	120	180	180	67
Third	10Hz	180	180	178	72
	12Hz	150	216	218	73
	15Hz	120	270	269	58

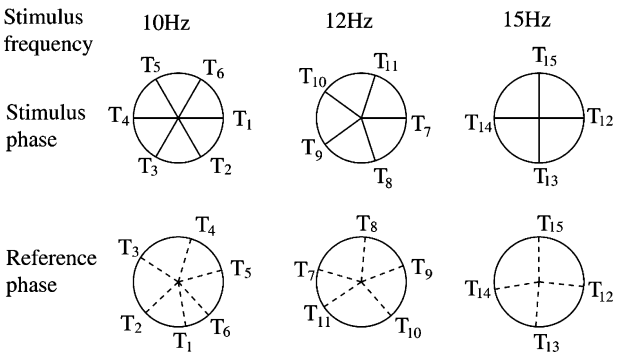

Fig. 7. Reference phases of a subject generated by stimuli with different phases. The solid lines represent the unit circles and the stimulus phases. Dotted lines represent the reference phases. $T_k\,(k = 1, 2, \ldots, 15)$ represent the targets, where the subject focused his attention to.

same frequency should be equally spaced in unit cycles as the stimulus phases. However, stimuli with equally spaced phases do not always generate equally spaced reference phases. Fig. 7 represents the reference phases of a subject when the 15 target stimuli at 10, 12, and 15 Hz were presented to him. The reference phases are calculated with data from the preliminary experiment, which usually results in unequal phase spacing.

Unequal intervals between reference phases influence the generalization performance of the classifier. Therefore, an extra treatment was required to recreate equally spaced reference phases.

The treatment contains following steps.

1) Obtain the reference phases measured under all the stimuli at a certain frequency.
2) Subtract the corresponding stimulus phases from the reference phases. Ideally, the results should be the same as reference phase of 0° stimulus, empirically there will be deviations.
3) Take the average of all the results from step 2 as the reference phase of 0° stimulus.
4) Add each stimulus phase to the reference phase from step 3 to get the new equally spaced reference phases. This equally spaced reference phases after the adjustment were called *calculated reference phases*.

The second and third harmonics follow the same procedure in order to be standardized.

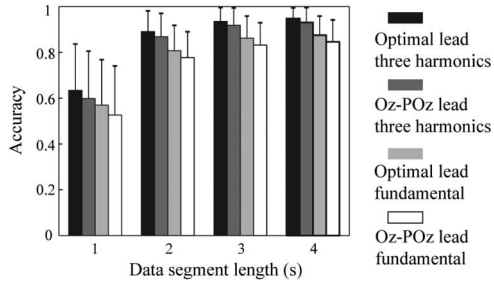

Fig. 8. Average discrimination accuracy under different data segment length for two different types of leads: optimal and Oz–POz.

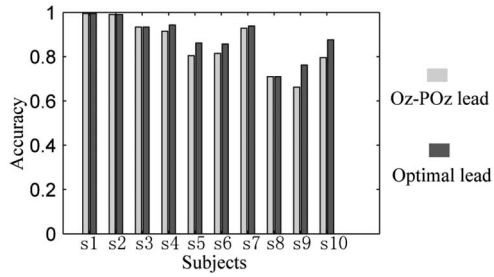

Fig. 9. Discrimination accuracy of different subjects at 2s data segment length using Oz–POz and optimal bipolar leads.

C. Discrimination Accuracy

In the offline experiment, we collected a total amount of 225 trials for each subject, among which the first 45 trials were for the preliminary experiment and the remaining 180 trials were used to calculate the discrimination accuracy.

Fig. 8 shows the subjects' average discrimination accuracy and the standard deviation versus data segment lengths for different types of bipolar leads.

In Fig. 8, it can be seen that when the data segment length increased from 1 to 2s, the average discrimination accuracy was greatly improved. However, when the data segment length increased from 2 to 4s, the improvement was relatively low.

While using the first three harmonics with a 2s data segment length and Oz–POz lead configuration, the average discrimination accuracy reached 85%; it could be further improved to 90% if the optimal lead was adopted.

Fig. 9 shows that four of the subjects (s1, s2, s3, and s8) achieved exactly the same accuracy from both lead configuration. This is because the optimal lead for these subjects is the Oz–POz (see Table I). Instead, for the other six subjects, the optimal lead configuration yielded a higher accuracy more or less. Though the adoption of the Oz–POz lead may affect the accuracy, but it avoids the time-consuming procedure of bipolar lead selection.

D. Simulated Online Experiment Results

We conducted a simulated online test with the offline data. According to the selected configuration of the offline experiment, the Oz–POz bipolar lead was adopted; all three harmonics of 2s data segment were used. We used the ITR proposed by Wolpaw *et al*. to evaluate the system performance [1]. In our study, the

TABLE III
SIMULATED ONLINE ITR

Subject	ITR(bit/min)	Subject	ITR(bit/min)
S1	89	S6	57
S2	90	S7	77
S3	78	S8	54
S4	79	S9	38
S5	45	S10	58

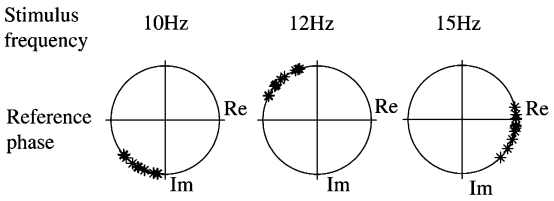

Fig. 10. Reference phases of stimulus of 0° at different frequencies for different subjects. The asterisk represents the calculated reference phase of 0° stimulus, while the solid line represents the unit circle and axes.

number of targets is 15. In the calculation of ITR, we assume that the data length of each trial is 2 s and there is 0.5 s rest time after each selection given to the subject to shift gaze to another target. We used the offline accuracy of 2s data segments for calculating a simulated ITR.

Table III shows the simulated ITR, which was calculated using the settings mentioned earlier.

The offline simulated ITR was 66.5 ± 18 bits/min. This ITR is comparable to the existing SSVEP-based BCI systems, which only use a frequency-coding method. Considering the complex situation in real application, the ITR in an online system may differ from our simulated results.

IV. DISCUSSION

A. Reference Phase of Different Subjects

The reference phases of the same stimulus vary amongst different subjects. Fig. 10 shows the calculated reference phases of SSVEP at the fundamental harmonic evoked by a stimulus of 0° for different subjects under different frequencies.

Fig. 10 shows that for the same stimulus, the reference phases of different subjects are different. For the stimuli of 0° at 10, 12, and 15 Hz, the standard deviations of reference phases are 16°, 18°, and 15°, respectively. These variations make it necessary to conduct a preliminary experiment to obtain the reference phase for each subject.

B. Response Latency

The reference phase of a 0° stimulus reflects SSVEP phase ($\phi_e(f_i)$). Using SSVEP phase, we can calculate SSVEP latency according to (2). For a subject, we can get several possible latency values with a different q selected under a specific stimulus frequency. However, SSVEP latency values under different stimulus frequencies should be similar. The possible response latencies for all subjects at different frequencies are shown in Fig. 11.

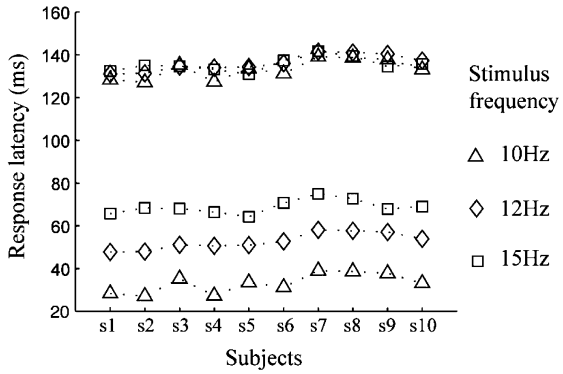

Fig. 11. SSVEP latency for the ten subjects in the offline experiment. In the lower part, q values for 10, 12, and 15 Hz are 0, 0, and 1, respectively. In the upper part, q values for 10, 12, and 15 Hz are 1, 1, and 2, respectively.

TABLE IV
DIFFERENCE BETWEEN MEASURED AND REFERENCE PHASES

Stimulus frequency	Standard deviation (°)	Confidence interval of 95% (°)
10 Hz	15	-29 ~ 29
12 Hz	16	-31 ~ 31
15 Hz	16	-31 ~ 31

From Fig. 11, we can see that similar SSVEP latencies of different stimulus frequencies are around 130 ms, which is in conformity with results of Di Russo and Spinelli [10], Falsini and Porciatti [11], and Johansson and Jakobsson [12].

C. Codable Targets at the Same Frequency

The difference between measured and reference phases can be understood as the human visual responses in different times. In the BCI applications, this variation may lead to faulty discrimination.

Table IV shows the distribution of difference between measured phases from test and reference phases from the preliminary experiment of all subjects at the fundamental component. The standard deviations and 95% confidence intervals of normal fitting are listed.

In order to correctly recognize the target, the difference should be limited within a certain range to avoid errors and confuse of one flicker's reference phase with the neighbors' reference phases. At a given frequency, the reference phase difference of fundamental component is $360°/M$, where M is the number of targets. Hence, the absolute difference between measured and reference phases should be smaller than $180°/M$. The confidence intervals of 95% of the distributions are $-29°\sim29°$, $-31°\sim31°$, and $-31°\sim31°$ respectively. Therefore, under a specific frequency, different phases should not code more than six targets.

V. Conclusion

In summary, we first used mixed phase and frequency coding in an SSVEP-based BCI to improve the ITR. The proposed system bears the following advantages.

First, it increases the number of codable targets under the same number of frequencies. With this method, we were able to code 15 targets by using only three frequencies on an LCD. The reference phase allows the identification of targets coded by phase at the same frequency.

Second, a BCI system with simple bipolar lead can reach a high ITR. The bipolar lead is a very convenient configuration for home BCI applications. Furthermore, this study proposed a commonly used bipolar lead Oz–POz, which increased the feasibility of BCI implementation.

The method of frequency and phase mixed coding could be useful for many computer-based applications, such as character input.

Future research will focus on reducing the time of preliminary experiment and conducting online experiment on a platform, which has already been developed.

Acknowledgment

The authors would like to thank Y. Wang, W. Wu, and D. Zhang for fruitful discussions and M. Gonzalez, L. Goldberg, A. Wisneski, and A. Ferrer for their language corrections.

References

[1] J. R. Wolpaw, N. Birbaumer, D. J. McFarland, G. Pfurtscheller, and T. M. Vaughan, "Brain–computer interfaces for communication and control," *Clin. Neurophysiol*, vol. 113, no. 6, pp. 767–791, 2002.

[2] M. Cheng, X. R. Gao, S. K. Gao, and D. Xu, "Design and implementation of a brain–computer interface with high transfer rates," *IEEE Trans. Biomed. Eng.*, vol. 49, no. 10, pp. 1181–1186, Oct. 2002.

[3] Y. J. Wang, R. P. Wang, X. R. Gao, B. Hong, and S. K. Gao, "A practical VEP-based brain–computer interface," *IEEE Trans. Neural Syst. Rehabil. Eng.*, vol. 14, no. 2, pp. 234–239, Jun. 2006.

[4] G. R. Muller-Putz and G. Pfurtscheller, "Control of an electrical prosthesis with an SSVEP-based BCI," *IEEE Trans. Biomed. Eng.*, vol. 55, no. 1, pp. 361–364, Jan. 2008.

[5] T. Kluge and M. Hartmann, "Phase coherent detection of steady-state evoked potentials: Experimental results and application to brain–computer interfaces," in *Proc. 3rd Int. IEEE EMBS Neural Eng. Conf.*, 2007, pp. 425–429.

[6] J. J. Wilson and R. Palaniappan, "Augmenting a SSVEP BCI through single cycle analysis and phase weighting," in *Proc. 4th Int. IEEE EMBS Conf. Neural Eng.*, Antalya, Turkey, 2009, pp. 371–374.

[7] Y. Wang, X. Gao, B. Hong, C. Jia, and S. Gao, "Brain-computer interfaces based on visual evoked potentials: Feasibility of practical system designs," *IEEE Eng. Med. Biol. Mag.*, vol. 27, no. 5, pp. 64–71, Sep./Oct. 2008.

[8] Z. Wu, Y. Lai, D. Wu, and D. Yao, "Stimulator selection in SSVEP-based BCI," *Med. Eng. Phys.*, vol. 30, no. 8, pp. 1079–1088, 2008.

[9] S. Moratti, B. A. Clementz, Y. Gao, T. Ortiz, and A. Keil, "Neural mechanisms of evoked oscillations: Stability and interaction with transient events," *Human Brain Mapp.*, vol. 28, no. 12, pp. 1318–1333, 2007.

[10] F. Di Russo and D. Spinelli, "Electrophysiological evidence for an early attentional mechanism in visual processing in humans," *Vis. Res.*, vol. 39, no. 18, pp. 2975–2985, 1999.

[11] B. Falsini and V. Porciatti, "The temporal frequency response function of pattern ERG and VEP: Changes in optic neuritis," *Electroencephalogr. Clin. Neurophysiol.*, vol. 100, no. 5, pp. 428–435, 1996.

[12] B. Johansson and P. Jakobsson, "Fourier analysis of steady-state visual evoked potentials in subjects with normal and defective stereo vision," *Documenta Ophthalmologica*, vol. 101, no. 3, pp. 233–246, 2000.

[13] H. Spekreijse, O. Estevez, and D. Reits, "Visual evoked potentials and the physiological analysis of visual processes in man," in *Visual Evoked Potentials in Man: New Developments*, J. E. Desmedt, Ed. Oxford, U.K.: Clarendon, 1977, pp. 16–89.

[14] H. Strasburger, "The analysis of steady state evoked potentials revisited," *Clin. Vis. Sci.*, vol. 1, no. 3, pp. 245–256, 1987.

[15] G. R. Muller-Putz, R. Scherer, C. Brauneis, and G. Pfurtscheller, "Steady-state visual evoked potential (SSVEP)-based communication: impact of harmonic frequency components," *Neural Eng.*, vol. 2, no. 4, pp. 123–130, 2005.

[16] A. Delorme and S. Makeig, "EEGLAB: An open source toolbox for analysis of single-trial EEG dynamics," *Neurosci. Methods*, vol. 134, no. 1, pp. 9–21, 2004.

Chuan Jia received the B.E. degree in biomedical engineering from Zhejiang University, Hangzhou, China, in 2004. He is currently working toward the Ph.D. degree in the Department of Biomedical Engineering, School of Medicine, Tsinghua University, Beijing, China.

His current research interests include brain–computer interface.

Xiaorong Gao (M'04) received the B.S. degree in biomedical engineering from Zhejiang University, Hangzhou, China, in 1986, the M.S. degree in biomedical engineering from Peking Union Medical College, China, in 1989, and the Ph.D. degree in biomedical engineering from Tsinghua University, Beijing, China, in 1992.

He is currently a Professor in the Department of Biomedical Engineering, Tsinghua University. His research interests include biomedical signal processing.

Bo Hong (M'04) received the B.E. and Ph.D. degrees in biomedical engineering from Tsinghua University, Beijing, China, in 1996 and 2001, respectively.

Since 2005, he has been an Associate Professor in the Department of Biomedical Engineering, School of Medicine, Tsinghua University, Beijing, China. His current research interests include neural information decoding and brain–computer interface.

Shangkai Gao (SM'94–F'07) received the B.S. degree in electrical engineering and the M.E. degree in biomedical engineering from the Department of Electrical Engineering, Tsinghua University, Beijing, China, in 1970 and 1982, respectively.

She is currently a Professor in the Department of Biomedical Engineering, Tsinghua University. Her research interests include brain–computer interface and medical imaging.

Prof. Gao is currently an Associate Editor of the IEEE Transactions on Biomedical Engineering and the Editorial Board Member of the *Journal of Neural Engineering*.